# Treatment Effect of Balloon Pulmonary Angioplasty in Chronic Thromboembolic Pulmonary Hypertension Quantified by Automatic Comparative Imaging in Computed Tomography Pulmonary Angiography

*Zhiwei Zhai, MS,* Hideki Ota, MD, PhD,† Marius Staring, PhD,* Jan Stolk, MD, PhD,‡ Koichiro Sugimura, MD, PhD,§ Kei Takase, MD, PhD,† and Berend C. Stoel, PhD**

**Objectives:** Balloon pulmonary angioplasty (BPA) in patients with inoperable chronic thromboembolic pulmonary hypertension (CTEPH) can have variable outcomes. To gain more insight into this variation, we designed a method for visualizing and quantifying changes in pulmonary perfusion by automatically comparing computed tomography (CT) pulmonary angiography before and after BPA treatment. We validated these quantifications of perfusion changes against hemodynamic changes measured with right-sided heart catheterization.

**Materials and Methods:** We studied 14 consecutive CTEPH patients (12 women; age, 70.5 ± 24), who underwent CT pulmonary angiography and right-sided heart catheterization, before and after BPA. Posttreatment images were registered to pretreatment CT scans (using the Elastix toolbox) to obtain corresponding locations. Pulmonary vascular trees and their centerlines were detected using a graph cuts method and a distance transform method, respectively. Areas distal from vessels were defined as pulmonary parenchyma. Subsequently, the density changes within the vascular centerlines and parenchymal areas were calculated and corrected for inspiration level differences. For visualization, the densitometric changes were displayed in color-coded overlays. For quantification, the median and interquartile range of the density changes in the vascular and parenchymal areas (ΔVD and ΔPD) were calculated. The recorded changes in hemodynamic parameters, including changes in systolic, diastolic, and mean pulmonary artery pressure (ΔsPAP, ΔdPAP, and ΔmPAP, respectively) and vascular resistance (ΔPVR), were used as reference assessments of the treatment effect. Spearman correlation coefficients were employed to investigate the correlations between changes in perfusion and hemodynamic changes.

**Results:** Comparative imaging maps showed distinct patterns in perfusion changes among patients. Within pulmonary vessels, the interquartile range of ΔVD correlated significantly with ΔsPAP ($R = -0.58$, $P = 0.03$), ΔdPAP ($R = -0.71$, $P = 0.005$), ΔmPAP ($R = -0.71$, $P = 0.005$), and ΔPVR ($R = -0.77$, $P = 0.001$). In the parenchyma, the median of ΔPD had significant correlations with ΔdPAP ($R = -0.58$, $P = 0.030$) and ΔmPAP ($R = -0.59$, $P = 0.025$).

**Conclusions:** Comparative imaging analysis in CTEPH patients offers insight into differences in BPA treatment effect. Quantification of perfusion changes provides noninvasive measures that reflect hemodynamic changes.

Received for publication May 28, 2017; and accepted for publication, after revision, November 11, 2017.

From the *Division of Image Processing, Department of Radiology, Leiden University Medical Center, Leiden, the Netherlands; †Department of Diagnostic Radiology, Tohoku University Hospital, Sendai, Japan; ‡Department of Pulmonology, Leiden University Medical Center, Leiden, the Netherlands; and §Department of Cardiology, Tohoku University Hospital, Sendai, Japan.

Correspondence to: Berend C. Stoel, PhD, Division of Image Processing, Department of Radiology, Leiden University Medical Center, PO Box 9600, 2300 RC, Leiden, the Netherlands. E-mail: b.c.stoel@lumc.nl.

Z. Zhai is supported by China Scholarship Council scholarship no. 201406120046. H. Ota is supported by Grant-in-Aid for Scientific Research (C) grant number JP16K10265.

Supplemental digital contents are available for this article. Direct URL citations appear in the printed text and are provided in the HTML and PDF versions of this article on the journal's Web site (www.investigativeradiology.com).

Copyright © 2017 Wolters Kluwer Health, Inc. All rights reserved.

ISSN: 0020-9996/17/0000–0000
DOI: 10.1097/RLI.0000000000000441

**Key Words:** chronic thromboembolic pulmonary hypertension, balloon pulmonary angioplasty, computed tomography, imaging quantifications

(*Invest Radiol* 2017;00: 00–00)

Chronic thromboembolic pulmonary hypertension (CTEPH) is caused by persistent obstruction of pulmonary arteries (PAs) after pulmonary embolism.[1] The mechanical obstruction of pulmonary arteries is produced by fibrotic transformation of pulmonary thrombus,[2] which could lead to pulmonary hypertension and increasing pulmonary vascular resistance (PVR). Without treatment, CTEPH patients have poor prognoses: 2 years of survival rate is less than 50% in patients with mean PA pressure (PAP) less than 30 mm Hg.[3,4] The prognosis can be improved by pulmonary endarterectomy[5] or balloon pulmonary angioplasty (BPA),[6] combined with optimal medications. Pulmonary endarterectomy is the curative treatment for CTEPH, with nearly normalized hemodynamics in the majority of patients.[7] However, for patients with inoperable CTEPH, BPA can be an alternative treatment to improve the clinical status and hemodynamics with a low mortality.[8]

Evaluation of disease severity and assessment of treatment effects play an important role in the therapy of CTEPH. In evaluating the severity of CTEPH and assessing treatment effects, invasive right-sided heart catheterization (RHC) serves as the criterion standard.[9] The 6-minute walk distance (6MWD)[10] and the brain natriuretic peptide (BNP) level[11] are the most frequently used noninvasive measurements to quantify treatment effect. Noninvasive imaging techniques play a key role in both diagnosis of CTEPH and assessment of the treatment effect.[2] Radionuclide ventilation/perfusion (VQ) scans are recommended as an initial step in the diagnosis of CTEPH,[9] but it is difficult to quantify treatment effects with VQ scans. Computed tomography (CT) pulmonary angiography (CTPA) is used in the evaluation of severity of CTEPH.[12] Compared with conventional pulmonary angiography, CTPA has benefits for providing additional details in high-resolution 3-D images.[13] Recently, dual-energy CT has shown its capability in visualizing pulmonary vascular disease and assessing severity of CTEPH.[14,15]

Balloon pulmonary angioplasty treatment can improve the hemodynamics of pulmonary vascular systems[8] and may contribute to the improvements of pulmonary vascular and parenchymal perfusion. We hypothesized that the perfusion changes achieved by BPA might reflect densitometric changes in CTPA. Thus, an objective and automatic method was designed to quantify the density changes in pulmonary vascular and parenchymal areas by comparatively analyzing CTPA before and after BPA. Moreover, we validated these image quantifications of perfusion changes against hemodynamic changes measured via RHC.

## MATERIALS AND METHODS

### Patients

We studied a cohort of 14 consecutive patients (age, 70.5 ± 24 years, including 12 women) who were diagnosed with inoperable CTEPH



Copyright © 2017 Wolters Kluwer Health, Inc. Unauthorized reproduction of this article is prohibited.
This paper can be cited using the date of access and the unique DOI number which can be found in the footnotes.

and were treated with BPA between May 2013 and April 2016, referred to the Tohoku University Hospital. All studied patients underwent both CTPA and RHC examinations, before and after BPA treatment. All patients underwent several sessions of BPA procedures besides standard medication such as anticoagulants and vasodilators. As a vasodilator for symptoms before BPA, Riociguat, Tadalafil, Ambrisentan, and Beraprost were used in 7, 5, 2, and 2 patients, respectively. During one procedure, the target lesion was limited to 1 or 2 segments in one lobe to minimize complications of BPA. We repeated BPA sessions at a 4- to 8-week interval.[6] Seven patients underwent the initial CTPA scan before the first BPA session; the other 7 subjects had undergone a part of BPA sessions before the initial CTPA scan. The number of BPA sessions between the 2 CTPA examinations ranged between 1 and 4 (median, 3). The intervals between CTPA and RHC were 0 to 37 days (median, 2 days). This prospective study was approved by the local ethics committee, and written informed consent was obtained from all patients.

All patients were scanned with a second-generation dual-source CT scanner (SOMATOM Definition Flash; Siemens Healthcare GmbH, Forchheim, Germany) with inspirational breath-hold and contrast enhancement. Contrast enhancement containing 350 mg/mL iodine was injected at a speed of 0.075 mL/kg per second × body weight (kg) over a period of 6 s, and subsequently a 40-mL saline flush was delivered at the same injection speed via a 20-gauge intravenous catheter, placed in the right antecubital vein using a double-headed power injector. A test injection technique was used to determine the scan delay: 12 mL of iodine-containing contrast medium followed by 20 mL of saline. For each patient, a region of interest was placed within the main PA and the time-density curve within the region of interest was recorded. The dual-source CT scan commenced 1 s after the test injection–mediated enhancement peaked.[15] The x-ray tube settings (with automatic tube current modulation) for tube A were 80 kVp with a quality reference mAs of 141, and the settings for tube B with a tin (Sn) filter were 140 kVp with a quality reference mAs of 60. The gantry rotation speed was 0.28 seconds per rotation; collimation, 64 × 0.6 mm; pitch, 1.00. Data were reconstructed with a slice thickness of 1 mm using a standard soft-tissue iterative reconstruction kernel (I30f, Sinogram Affirmed Iterative Reconstruction [SAFIRE], strength 3). The 80 and 140 kVp images were fused into mixed images with a single energy of 120 kVp and with a mixing ratio of 0.6:0.4, using the dual-energy application software on a commercially available workstation (syngo CT Workplace, VA44A; Siemens Healthcare GmbH).[15] Only the mixed CTPA images were investigated in this study.

The hemodynamic parameters were examined at the main PA via RHC in all patients both before and after BPA treatment. These included PAP (systolic, diastolic, and mean), systolic right ventricular pressure, right atrial pressure, cardiac output (CO), cardiac index (CI), and pulmonary capillary wedge pressure (PCWP). The PVR was calculated using the following formula: PVR = (mean PAP − PCWP)/CO × 80 (dyne·s/cm$^5$).[16] The RHC examinations were used as the criterion standard to evaluate the severity of CTEPH;[9] the changes in PAP (ΔsPAP, ΔdPAP, and ΔmPAP) and in PVR (ΔPVR) after BPA treatment were calculated as the reference assessments for the treatment effects. The 6MWD data were recorded for 13 of 14 patients. Brain natriuretic peptide and mean transit time (MTT) were collected for all patients. The diameter of the PA trunk was measured on axial images. Short axis measurements of the left and right ventricle (LV and RV, respectively) were performed in 4-chamber images, and the ratio between RV and LV short axes (RV/LV) was calculated. The interventricular septum was assessed on the midchamber short axis images. Interventricular septal angle (ISA) was measured by determining the angle between the midpoint of the interventricular septum and the 2 hinge points. These CT measurements were performed on a commercially available workstation (Aquarius Net; TeraRecon, San Mateo, CA).

## Image Analysis

Computed tomography pulmonary angiography scans were preprocessed with lung volume segmentation using multiatlas-based methods. Three atlases that were labeled semiautomatically by pulmonary experts using Pulmo-CMS software[17] were registered to each CTPA scan with Elastix.[18] Majority voting was used to fuse the labels and extract the final lung segmentation. Pulmonary vessels were extracted within the lung volume using a graph cuts–based method,[19] where the vessel likelihood (so-called vesselness, measured by the strain energy filter[20]) and CT intensity were combined into a single cost function. Both PAs and veins were included as the entire pulmonary vascular trees.

For each patient, pairwise image registration was employed between CT images of post- and pre-BPA, using Elastix, as reported previously.[21] The volume correction in this method was originally designed for parenchymal areas only, as a measure to correctly assess emphysema progression, where a proportional local increase in volume (estimated by the determinant of the Jacobian) was compensated by a proportional decrease in density (called the "dry sponge model"):

$$\Delta D(x) = I_{\text{post}}(T(x)) - I_{\text{pre}}(x) \cdot [\det \mathbf{J}_T(x)]^{-1} \quad (1)$$

where $\Delta D(x)$ is the estimated density change at position $x$; $I_{\text{pre}}(x)$ and $I_{\text{post}}(x)$ are the image intensities of the pre- and post-BPA CT scan; $T(x)$ is the transformation function from the image registration, mapping the coordinate $x$ in the pre-BPA scan to the corresponding position in the post-BPA scan; and $\det \mathbf{J}_T(x)$ is the determinant of the Jacobian of the transformation field at position $x$.

Because the "dry sponge model" is not applicable to the pulmonary areas with high density, where pure liquid in pulmonary vessels is not compressible, we modified the model to restrict the scaling factor ($\det \mathbf{J}_T(x)$) depending on the density. This so-called restricted sponge model considers a voxel as composed of 2 components, air and liquid. Then density can be increased by leaving out the air component, and the density is only allowed to decrease by a maximum of 4 times the original volume of the air component (Fig. 1A). This means that the scaling factor is allowed to range from 0 to 4 if a voxel contains only air. For a voxel containing 100% water, blood, or a contrast agent (ie, densities higher than 1000 g/L) that is not compressible, the scaling factor is set to 1. And for voxels with original densities between 0 and 1000 g/L, linear lower and upper bounds for the scaling factor are used (Fig. 1B). Therefore, the sponge model in Eq (1) was modified as follows:

$$\Delta D(x) = I_{\text{post}}(T(x)) - I_{\text{pre}}(x) \cdot \max\{\theta_{\min}(I_{\text{pre}}(x)),\ \min\{\theta_{\max}(I_{\text{pre}}(x)),\ \det \mathbf{J}_T(x)\}\}^{-1} \quad (2)$$

where $\theta_{\min}$ and $\theta_{\max}$ are the linear lower and upper bound, respectively.

To eliminate the dependence on a perfect matching quality between follow-up and baseline at the vascular boundary regions, we extracted only the centerlines of vessels by the symmetric distance transform method (DtSkeletonization method of Mevislab 2.7[22]). Subsequently, only the voxels on the vascular centerlines were used for quantifying the density changes, which were estimated with Eq (2). For visualization, the "densitometric change" map was displayed as color-coded overlays as shown in Figure 2, A and D, and 3-D color-coded vascular centerlines were generated, as illustrated in Figure 2, B and E. For quantification, the median and interquartile range (IQR) of the vascular densitometric changes (ΔVD) were calculated, as shown in Figure 2,C and F, which were used to quantify the perfusion changes within vessels. The densitometric changes in parenchyma (ΔPD) were


© 2017 Wolters Kluwer Health, Inc. All rights reserved.

Copyright © 2017 Wolters Kluwer Health, Inc. Unauthorized reproduction of this article is prohibited.
This paper can be cited using the date of access and the unique DOI number which can be found in the footnotes.

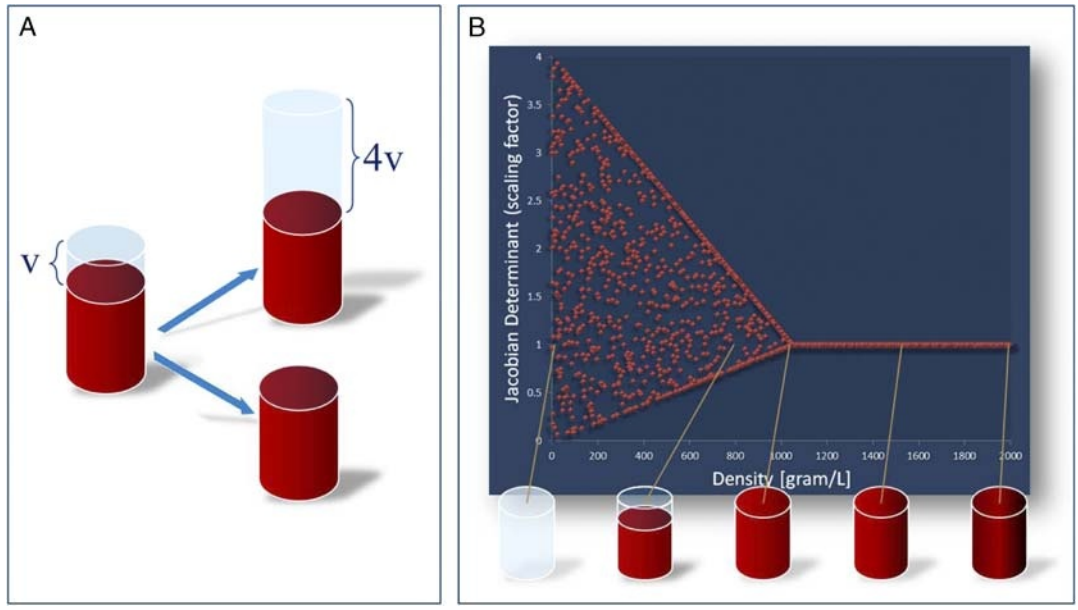


**FIGURE 1.** A, Two-component model: a voxel is composed of an air and blood compartment (or water or contrast agent), where density increase is restricted to the situation where all air has been expired, or where there is a 4-fold increase of the amount of inspired air. B, The scaling factor from the determinant of the Jacobian is thus restricted by an upper and lower limit depending on the density of a voxel. Figure 1 can be viewed online in color at www.investigativeradiology.com.

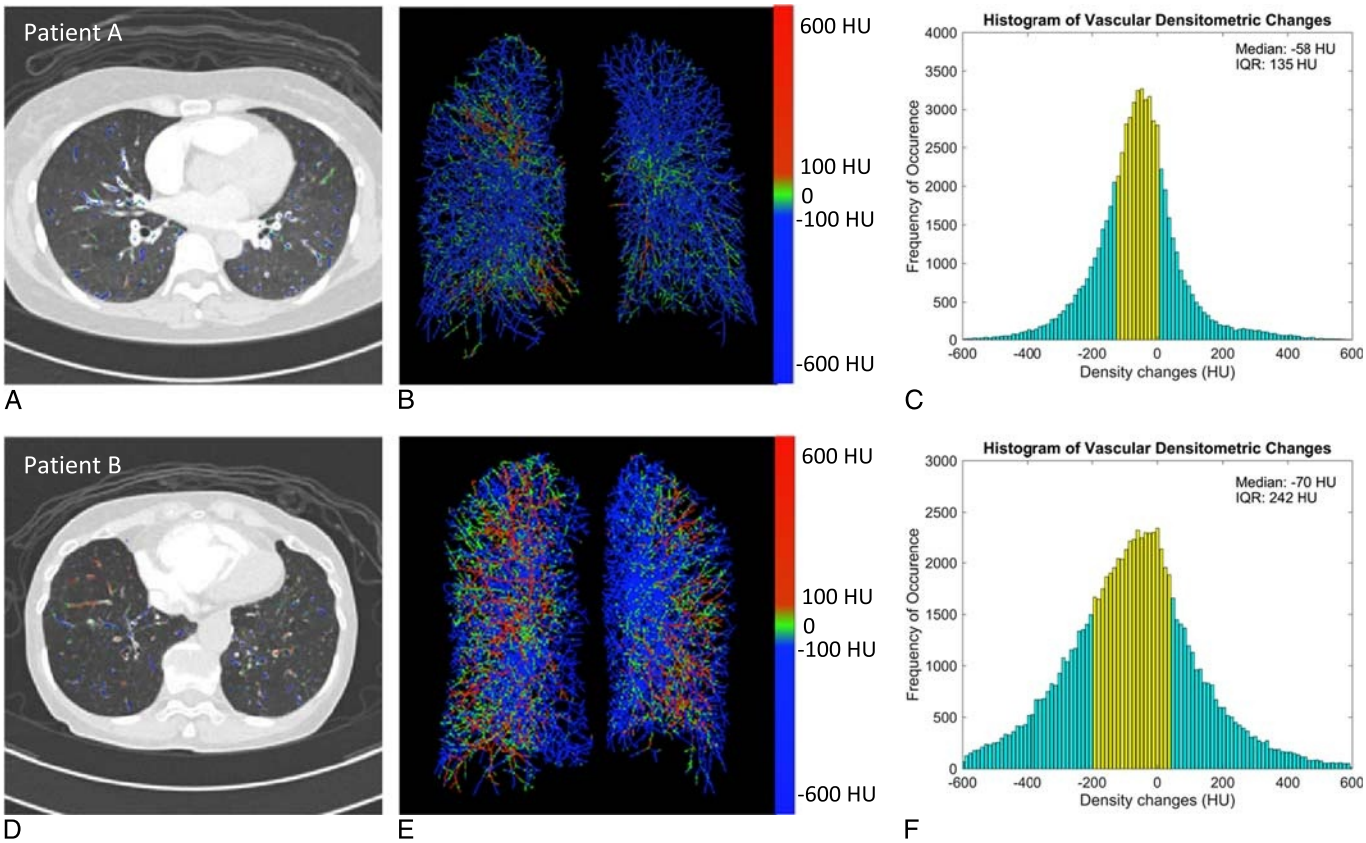


**FIGURE 2.** Vascular densitometric changes of 2 patients. A and D, One slice of CTPA with color-coded overlay of vascular densitometric changes. B and E, 3-D color-coded visualization of vascular centerlines. C and F, Histogram of vascular densitometric changes and yellow bins representing vascular densitometric changes within the IQR. Patient A and B had a decrease in mPAP by −3 and −34 mm Hg, respectively, and a decrease in PVR by −39 and −734 dyne·s/cm$^5$, respectively. Figure 2 can be viewed online in color at www.investigativeradiology.com.

*© 2017 Wolters Kluwer Health, Inc. All rights reserved.*



Copyright © 2017 Wolters Kluwer Health, Inc. Unauthorized reproduction of this article is prohibited.
This paper can be cited using the date of access and the unique DOI number which can be found in the footnotes.

**TABLE 1.** Changes in Hemodynamic Parameters, 6MWD, BNP, MTT, RV/LV Ratio, PA Diameter, ISA, and Densitometry

| | Pre-BPA | Post-BPA | Change | *P* |
|---|---|---|---|---|
| RHC parameters | | | | |
| sPAP (mm Hg) | 60.5 ± 33 | 36 ± 19 | 23 ± 19 | 0.002 |
| dPAP (mm Hg) | 20 ± 16 | 12.5 ± 11 | −5 ± 11 | 0.006 |
| mPAP (mm Hg) | 34.5 ± 17 | 21.5 ± 15 | −12.5 ± 14 | 0.003 |
| PVR (dyne·s/cm$^5$) | 496 ± 396 | 246 ± 185 | −185 ± 409 | 0.004 |
| 6MWD (m) | 450 ± 159 | 510 ± 95 | 50 ± 115 | 0.004 |
| BNP (pg/mL) | 80.4 ± 160 | 26.8 ± 32.7 | −53.2 ± 146 | 0.01 |
| MTT (s) | 10.1 ± 2.95 | 9.95 ± 2.1 | −0.05 ± 2.08 | 0.31 |
| RV/LV ratio | 1.21 ± 0.53 | 1.05 ± 0.1 | −0.09 ± 0.28 | 0.005 |
| PA diameter (mm) | 30.1 ± 6.22 | 28.6 ± 5.54 | −1.9 ± 3.43 | 0.024 |
| ISA (degree) | 131 ± 11.8 | 130 ± 16.2 | −2.5 ± 27.5 | 0.397 |
| Density measurements (HU) | | | | |
| Median VD | −415 ± 101 | −433 ± 114 | −51.5 ± 20.8 | <0.001 |
| IQR of VD | 437 ± 73 | 475 ± 67 | 182 ± 60 | <0.001 |
| Median PD | −864 ± 47 | −861 ± 54 | −3.5 ± 22.5 | 0.379 |
| IQR of PD | 437 ± 73 | 475 ± 67 | 45 ± 15 | <0.001 |

See the online supplement, Supplemental Digital Content 1, http://links.lww.com/RLI/A364, for individual measurement results.

BPA indicates balloon pulmonary angioplasty; sPAP, systolic pulmonary artery pressure; dPAP, diastolic pulmonary artery pressure; mPAP, mean pulmonary artery pressure; 6MWD, 6-minute walk distance; BNP, brain natriuretic peptide; MTT, mean transit time; RV/LV ratio, right ventricular short axis to left ventricular short axis ratio; PA diameter, diameter of pulmonary artery trunk; ISA, interventricular septal angle; VD, vascular density; PD, parenchymal density.

measured at the location of parenchymal "centerlines," which were the parenchymal areas distal to pulmonary vessels. Similarly, the perfusion changes in pulmonary parenchyma were quantified by the median and IQR of the ΔPD.

### Statistical Analysis

Continuous variables of the patient characteristics are presented as median and IQR, and categorical variables are presented as frequencies and percentages. The normality of each variable was tested with a Shapiro-Wilk test and a normal Q-Q plot. The changes in RHC parameters, 6MWD, BNP levels, MTT, RV/LV ratio, PA diameter, ISA, and density measurements between pre- and post-BPA were tested using the paired *t* test or the Wilcoxon signed-rank test, as appropriate. Correlations between hemodynamic changes, 6MWD, BNP, and densitometric changes were evaluated using Spearman correlation coefficient. All statistical computations were performed in SPSS (Version 20.0; IBM Corp, Armonk, NY). A 2-tailed *P* value less than 0.05 was considered to be statistically significant.

## RESULTS

The changes in RHC parameters, 6MWD, BNP, MTT, RV/LV ratio, PA diameter, ISA, and perfusional quantifications between pre- and post-BPA are shown in Table 1. The hemodynamic parameters were improved by the BPA treatment, with a statistically significant decrease in sPAP, dPAP, mPAP, and PVR. The 6MWD, BNP, RV/LV ratio, and PA diameter were also significantly improved by the BPA treatment. The median densities decreased within the vascular trees after BPA, as quantified by automatic comparative imaging analysis (Table 1). In the parenchyma on the other hand, the median densities did not change significantly.

The results of Spearman correlation analysis between change in RHC parameters and change in densities are provided in Table 2. The IQR of ΔVD was significantly negatively correlated with all RHC parameters: ΔsPAP ($R = -0.58$, $P = 0.03$), ΔdPAP ($R = -0.71$, $P = 0.005$), ΔmPAP ($R = -0.71$, $P = 0.005$), and ΔPVR ($R = -0.77$, $P = 0.001$), which indicates that a wider IQR of ΔVD histogram corresponds to a larger decrease in both PAP and PVR after BPA treatment. Scatter plots of the hemodynamic changes and IQR of ΔVD are presented in Figure 3, among which the significant association between ΔPVR and IQR of ΔVD was particularly strong. Besides, the median of ΔPD was significantly correlated with both ΔdPAP ($R = -0.58$, $P = 0.030$) and ΔmPAP ($R = -0.59$, $P = 0.025$), which implies that the perfusion changes of pulmonary parenchyma could partly reflect the hemodynamic parameter changes. The Δ6MWD was significantly correlated with the median of ΔVD ($R = -0.67$, $P = 0.012$), and ΔBNP had a significant correlation with the IQR of ΔPD ($R = -0.645$, $P = 0.013$).

## DISCUSSION

We studied the pulmonary perfusion changes in CTPA of CTEPH patients before and after BPA treatment. The CTPA before and after BPA treatment were compared by an automatic and objective method for identifying the perfusion changes in pulmonary vessels and parenchyma. The median and IQR of perfusion changes in pulmonary vessels and parenchyma were validated against RHC parameter changes. The IQR of ΔVD were significantly correlated with all PAP measurements and PVR, indicating that the hemodynamic changes could be

**TABLE 2.** Correlation *R* (*P* Value) Analysis Between RHC Parameters, 6MWD, BNP, and Image-Derived Perfusion Changes

| | Median of ΔVD | IQR of ΔVD | Median of ΔPD | IQR of ΔPD |
|---|---|---|---|---|
| ΔsPAP | 0.53 (0.054) | −0.58 (0.031) | −0.32 (0.263) | −0.18 (0.529) |
| ΔdPAP | 0.18 (0.536) | −0.71 (0.005) | −0.58 (0.030) | −0.40 (0.152) |
| ΔmPAP | 0.46 (0.095) | −0.71 (0.005) | −0.59 (0.025) | −0.37 (0.190) |
| ΔPVR | 0.28 (0.325) | −0.77 (0.001)* | −0.43 (0.121) | −0.36 (0.201) |
| Δ6MWD | −0.67 (0.012) | −0.011 (0.817) | −0.011 (0.971) | 0.48 (0.093) |
| ΔBNP | 0.10 (0.725) | −0.53 (0.052) | −0.39 (0.163) | −0.65 (0.013) |

For quantification, the median and interquartile range of the density changes in the vascular and parenchymal areas (ΔVD and ΔPD) were calculated.

*Significance level obtained after Bonferroni correction for multiple testing.

VD indicates vascular density; PD, parenchymal density; sPAP, systolic pulmonary artery pressure; PVR, pulmonary vascular resistance; 6MWD, 6-minute walk distance; BNP, brain natriuretic peptide.


© 2017 Wolters Kluwer Health, Inc. All rights reserved.

Copyright © 2017 Wolters Kluwer Health, Inc. Unauthorized reproduction of this article is prohibited.
This paper can be cited using the date of access and the unique DOI number which can be found in the footnotes.

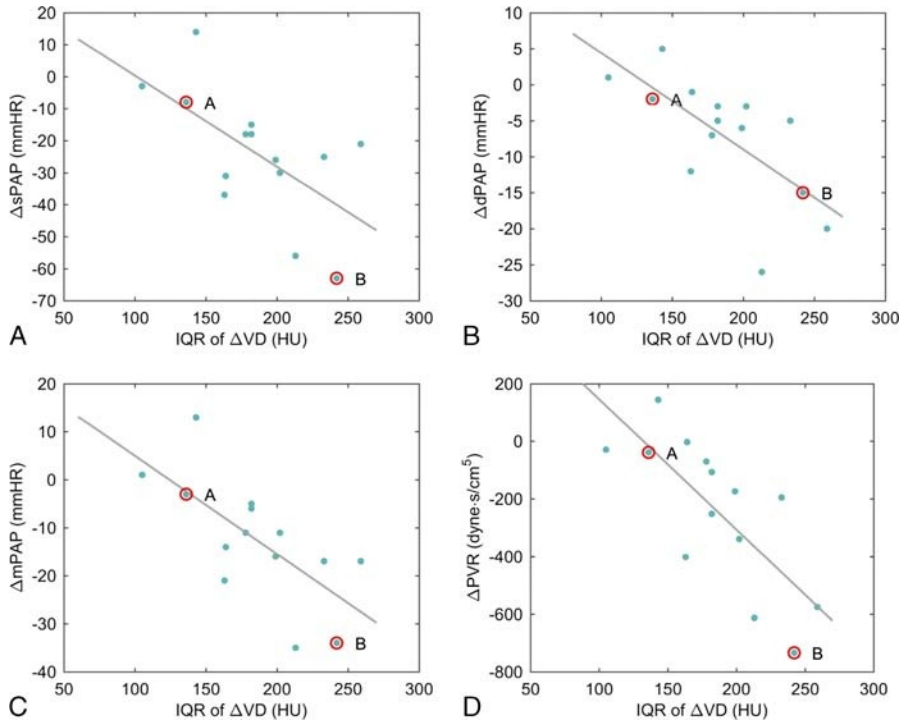


**FIGURE 3.** Correlation between IQR of ΔVD and RHC parameters (A and B correspond to patient A and B in Fig. 2, respectively). A, Correlation between IQR of ΔVD and Δ*s*PAP ($R = -0.58$, $P = 0.031$). B, Correlation between IQR of ΔVD and ΔdPAP ($R = -0.71$, $P = 0.005$). C, Correlation between IQR of ΔVD and ΔmPAP ($R = -0.71$, $P = 0.005$). D, Correlation between IQR of ΔVD and ΔPVR ($R = -0.77$, $P = 0.001$). Figure 3 can be viewed online in color at www.investigativeradiology.com.

reflected by perfusion changes. Furthermore, the color-coded visualization can offer insight into localized differences in BPA treatment effect.

The variety in perfusion changes in pulmonary vessels was quantitatively assessed by IQR of ΔVD, as it reflects the spread of both decrease and increase in density within pulmonary vessels. Vessels proximal to an obstruction ("upstream vessels") react differently to BPA treatment than vessels distal to an obstruction ("downstream vessels"). Because of the obstructions in PAs before treatment, contrast medium would accumulate in the "upstream vessels" where hypertension leads to dilation and increased density in CTPA. The "downstream vessels," however, are initially not reached by contrast medium, and their densities in CTPA would therefore be lower than normal. When obstructions have been treated by BPA, the distribution of contrast medium through the pulmonary vascular system may be normalized. Therefore, the contrast medium is distributed more homogeneously after BPA, that is, the densities in "upstream vessel" would have decreased and the densities in "downstream vessels" would have increased after treatment. Thus, a wider range in ΔVD implies more equalization of contrast medium in vessels, that is, more hemodynamic improvements.

To demonstrate the visualization of the changes in the quantified parameters, 2 patients with different outcomes after BPA were selected. According to RHC assessments, patient B had a larger decline in PAP and PVR after BPA treatment in comparison with patient A. As shown in the histogram of vascular densitometric changes, the IQR of patient B is wider than that of patient A. In the color-coded 2-D visualization (Fig. 2A, D), most of the vascular tree in patient A is coded in green, whereas in patient B, more blue- and red-coded vessels are displayed. This implies that perfusion changes in patient B are more widely spread, that is, a better treatment effect.

In the pulmonary parenchyma, the hemodynamic changes obtained from RHC were reflected by the median ΔPD, not by the IQR of ΔPD. Because of the poor performance of the pulmonary vascular system before BPA treatment, transport of contrast medium to the parenchymal areas may be limited. After the BPA treatment, the performance of the vascular system might have been improved. Thus, instead of the variation in ΔPD, the median of ΔPD will provide insights into the perfusion changes in pulmonary parenchyma. The median of ΔPD was not significantly different from 0, although it was significantly correlated with ΔdPAP and ΔmPAP. The median of ΔPD did not change on average; however, its increases/decreases in an individual patient might moderately reflect the changes in RHC parameters. Although the information from ΔPD quantifications is not as clear as that from ΔVD, investigating changes in the pulmonary parenchyma shows potential.

Recently, several studies demonstrated the significant treatment effect of BPA by cautiously limiting the number of balloon inflations and target segments per session, thus reducing the incidence of adverse complications, such as reperfusion edema and pulmonary bleeding.[1] This procedure was added to treatment algorithms in the ESC/ERS guideline.[23] However, its efficacy for long-term prognosis has not been established yet. In our clinical setting as an experienced CTEPH center, though rare, there are patients demonstrating reexacerbation of CTEPH, year(s) after completion of BPA treatment courses. Considering the features of BPA procedure and patients' clinical course, several follow-ups are necessary in the management of patients with CTEPH. Our results provided objective and quantitative changes of pulmonary perfusion after BPA along with densitometry information on CTPA, which were correlated with invasive RHC examinations.

Some previous studies have reported methods for estimating the severity of CTEPH. A study[24] validated automatic quantification of pulmonary perfused blood volume (PBV) with CI, PAP, PVR, and 6MWD in 25 CTEPH patients. The PBV had negative significant

© 2017 Wolters Kluwer Health, Inc. All rights reserved.


Copyright © 2017 Wolters Kluwer Health, Inc. Unauthorized reproduction of this article is prohibited.
This paper can be cited using the date of access and the unique DOI number which can be found in the footnotes.

correlations with sPAP and mPAP, but not significant with PVR, CI, and 6MWD. In another study,[15] authors manually measured lung PBV to correct the influence of artifacts and evaluated the PBV with PAP, PVR, and right ventricular pressure for 46 CTEPH patients. The lung PBV was significantly correlated with sPAP, dPAP, mPAP, and PVR. The manually measured PBV might be used as a noninvasive estimator of clinical CTEPH severity; however, reproducibility and objectivity of manual visual evaluations are generally poor. The pulmonary vascular morphology was investigated as an imaging biomarker for CTEPH in a recent study,[25] in which the ratio of small-vessel volume (blood volume of vessels with a cross-sectional area of ≤5 $mm^2$, BV5) and total blood vessel volume (TBV) was measured for small-vessel pruning, and the ratio of large-vessel volume (a cross-sectional area of >10 $mm^2$, BV >10) and TBV was quantified for large-vessel dilation. The measurements were extracted in CTPA for 18 patients with CTEPH and 15 control patients. The quantifications of BV5/TBV and BV >10/TBV were significantly different between the CTEPH and the control group, implying that pulmonary vascular morphology was remodeled by CTEPH. The pulmonary vascular morphology may be used as an imaging biomarker to assess disease severity. In another study,[26] the lung PBV was quantified by dual-energy CT in 8 female patients with CTEPH pre- and post-BPA treatment and corrected with PA enhancement (lung PBV/PAenh). The pre- to post-BPA improvements PBV/PAenh of both lungs had significant positive correlations with PAP, PVR, and 6MWD, which implied that the lung PBV might be an indicator of BPA treatment effect. Optical coherence tomography was used to classify the morphologies of 43 lesions in 17 patients pre- and post-BPA in another study.[27] The newly proposed optical coherence tomography–based morphological lesion classification was evaluated to the pressure ratio and compared with conventional angiographic findings, which proved to be promising to predict accurate estimation of lesion responsiveness to BPA. In this study, the IQR of ΔVD can be used as a measurement to assess the treatment effect and additionally offers color-coded visualization back to CTPA. Furthermore, we compared CTPA before and after treatment, which offers insight into the treatment effect.

There are some limitations in our study. The quantifications were performed on both lungs together. More specific analysis of separate lungs or lung lobes may provide a more localized and accurate assessment of perfusion changes. We did not obtain an echocardiogram or magnetic resonance imaging data along with the CT examination to evaluate CO. The postcontrast attenuation was not normalized for intraindividual variations that might be influenced by CO. In the present study, the arteries and veins were not analyzed separately with an automatic method, whereas perfusion changes may differ between arteries and veins. A separated analysis of arteries and veins may therefore further improve the correlation. Nevertheless, even without these particular analyses, we already found a highly significant association between perfusion changes and hemodynamic changes. In the future, quantifying the vessels with lesions treated by BPA would be an interesting research topic, as automatic and objective quantifications of the lesion morphology could provide specific benefits for planning or assessing BPA treatment. The studied group was relatively small and only included CTEPH patients without a control group. The normal vascular perfusion in healthy people might contribute to enhance the understanding of relations between pulmonary vascular perfusion and hemodynamic parameters. However, the method still offers insight into the variance in BPA treatment effects.

In conclusion, PAP and PVR were significantly improved after BPA in the studied patient group with inoperable CTEPH. We assessed the perfusion changes in pulmonary vasculature achieved by BPA using an automatic comparison of CTPAs acquired before and after treatment. The IQR of ΔVD is associated with hemodynamic changes and can be used as a noninvasive measurement for assessing BPA treatment effects. The color-coded visualization provides insight into local differences in BPA treatment effects.

## ACKNOWLEDGEMENTS

*We would like to acknowledge Wenyu Sun for measuring the cardiac output parameters, Baldur van Lew for reviewing the English grammar, and Ningning Xu for reviewing the statistical analyses.*

## REFERENCES

1. Hoeper MM, Mayer E, Simonneau G, et al. Chronic thromboembolic pulmonary hypertension. *Circulation*. 2006;113:2011–2020.
2. Lang IM, Madani M. Update on chronic thromboembolic pulmonary hypertension. *Circulation*. 2014;130:508–518.
3. Lewczuk J, Piszko P, Jagas J, et al. Prognostic factors in medically treated patients with chronic pulmonary embolism. *Chest*. 2001;119:818–823.
4. Riedel M, Stanek V, Widimsky J, et al. Longterm follow-up of patients with pulmonary thromboembolism: late prognosis and evolution of hemodynamic and respiratory data. *Chest*. 1982;81:151–158.
5. Mayer E, Jenkins D, Lindner J, et al. Surgical management and outcome of patients with chronic thromboembolic pulmonary hypertension: results from an international prospective registry. *J Thorac Cardiovasc Surg*. 2011;141:702–710.
6. Sugimura K, Fukumoto Y, Satoh K, et al. Percutaneous transluminal pulmonary angioplasty markedly improves pulmonary hemodynamics and long-term prognosis in patients with chronic thromboembolic pulmonary hypertension. *Circ J*. 2012;76:485–488.
7. Madani MM, Auger WR, Pretorius V, et al. Pulmonary endarterectomy: recent changes in a single institution's experience of more than 2,700 patients. *Ann Thorac Surg*. 2012;94:97–103.
8. Mizoguchi H, Ogawa A, Munemasa M, et al. Refined balloon pulmonary angioplasty for inoperable patients with chronic thromboembolic pulmonary hypertension. *Circ Cardiovasc Interv*. 2012;5:748–755.
9. Kim NH, Delcroix M, Jenkins DP, et al. Chronic thromboembolic pulmonary hypertension. *J Am Coll Cardiol*. 2013;62(suppl 25):D92–D99.
10. Reesink HJ, van der Plas MN, Verhey NE, et al. Six-minute walk distance as parameter of functional outcome after pulmonary endarterectomy for chronic thromboembolic pulmonary hypertension. *J Thorac Cardiovasc Surg*. 2007;133:510–516.
11. Reesink HJ, Tulevski II, Marcus JT, et al. Brain natriuretic peptide as noninvasive marker of the severity of right ventricular dysfunction in chronic thromboembolic pulmonary hypertension. *Ann Thorac Surg*. 2007;84:537–543.
12. Liu M, Ma Z, Guo X, et al. Computed tomographic pulmonary angiography in the assessment of severity of chronic thromboembolic pulmonary hypertension and right ventricular dysfunction. *Eur J Radiol*. 2011;80:e462–e469.
13. Ley S, Ley-Zaporozhan J, Pitton MB, et al. Diagnostic performance of state-of-the-art imaging techniques for morphological assessment of vascular abnormalities in patients with chronic thromboembolic pulmonary hypertension (CTEPH). *Eur Radiol*. 2012;22:607–616.
14. Krissak R, Henzler T, Reichert M, et al. Enhanced visualization of lung vessels for diagnosis of pulmonary embolism using dual energy CT angiography. *Invest Radiol*. 2010;45:341–346.
15. Takagi H, Ota H, Sugimura K, et al. Dual-energy CT to estimate clinical severity of chronic thromboembolic pulmonary hypertension: comparison with invasive right heart catheterization. *Eur J Radiol*. 2016;85:1574–1580.
16. Fuster V. *Hurst's the Heart*. New York, NY: McGraw-Hill Medical; 2008.
17. Stoel BC, Stolk J. Optimization and standardization of lung densitometry in the assessment of pulmonary emphysema. *Invest Radiol*. 2004;39:681–688.
18. Klein S, Staring M, Murphy K, et al. Elastix: a toolbox for intensity-based medical image registration. *IEEE Trans Med Imaging*. 2010;29:196–205.
19. Zhai Z, Staring M, Stoel BC. Lung vessel segmentation in CT images using graph cuts. In: *SPIE Medical Imaging*. San Diego, CA: International Society for Optics and Photonics: 97842K-K-8; 2016.
20. Xiao C, Staring M, Shamonin D, et al. A strain energy filter for 3D vessel enhancement with application to pulmonary CT images. *Med Image Anal*. 2011;15:112–124.
21. Staring M, Bakker ME, Stolk J, et al. Towards local progression estimation of pulmonary emphysema using CT. *Med Phys*. 2014;41:021905.
22. Selle D, Preim B, Schenk A, et al. Analysis of vasculature for liver surgical planning. *IEEE Trans Med Imaging*. 2002;21:1344–1357.


© 2017 Wolters Kluwer Health, Inc. All rights reserved.

Copyright © 2017 Wolters Kluwer Health, Inc. Unauthorized reproduction of this article is prohibited.
This paper can be cited using the date of access and the unique DOI number which can be found in the footnotes.

23. Galiè N, Humbert M, Vachiery JL, et al. 2015 ESC/ERS guidelines for the diagnosis and treatment of pulmonary hypertension. *Eur Heart J*. 2016;37:67–119.
24. Meinel F, Graef A, Thierfelder K, et al. Automated quantification of pulmonary perfused blood volume by dual-energy CTPA in chronic thromboembolic pulmonary hypertension. *RöFo*. 2014;186. 151–156.
25. Rahaghi F, Ross JC, Agarwal M, et al. Pulmonary vascular morphology as an imaging biomarker in chronic thromboembolic pulmonary hypertension. *Pulm Circ*. 2016;6:70–81.
26. Koike H, Sueyoshi E, Sakamoto I, et al. Quantification of lung perfusion blood volume (lung PBV) by dual-energy CT in patients with chronic thromboembolic pulmonary hypertension (CTEPH) before and after balloon pulmonary angioplasty (BPA): preliminary results. *Eur J Radiol*. 2016;85: 1607–1612.
27. Inohara T, Kawakami T, Kataoka M, et al. Lesion morphological classification by OCT to predict therapeutic efficacy after balloon pulmonary angioplasty in CTEPH. *Int J Cardiol*. 2015;197:23–25.

*© 2017 Wolters Kluwer Health, Inc. All rights reserved.*


Copyright © 2017 Wolters Kluwer Health, Inc. Unauthorized reproduction of this article is prohibited.
This paper can be cited using the date of access and the unique DOI number which can be found in the footnotes.